ESC European Society of Cardiology

Cardiovascular Research
doi:10.1093/cvr/cvz259

Development of a new mouse model for coxsackievirus-induced myocarditis by attenuating coxsackievirus B3 virulence in the pancreas

Sandra Pinkert[1,2†], Markian Pryshliak[1†], Kathleen Pappritz[3,4], Klaus Knoch[5], Ahmet Hazini[1], Babette Dieringer[1], Katrin Schaar[1], Fengquan Dong[4], Luisa Hinze[1], Jie Lin[4], Dirk Lassner [6], Robert Klopfleisch[7], Michele Solimena[5], Carsten Tschöpe [8], Ziya Kaya[9], Muhammad El-Shafeey[3,10], Antje Beling [2], Jens Kurreck [1], Sophie Van Linthout[3,4,8], Karin Klingel[11†], and Henry Fechner [1*†]

[1]Department of Applied Biochemistry, Institute of Biotechnology, Technische Universität Berlin, Gustav-Meyer-Allee 25, 15533 Berlin, Germany; [2]Charité - Universitätsmedizin Berlin, corporate member of Freie Universität Berlin, Humboldt-Universität zu Berlin, and Berlin Institute of Health (BIH), Institute of Biochemistry, Virchowweg 6, 10117 Berlin, Germany; [3]Berlin—Brandenburger Center for Regenerative Therapies (BCRT), Charité—Universitätsmedizin Berlin, Campus Virchow Klinikum (CVK), Föhrer Str. 15, 13353 Berlin, Germany; [4]German Center for Cardiovascular Research (DZHK), Partner Site Berlin—Charité, Oudenarder Straße 16, 13316 Berlin, Germany; [5]Faculty of Medicine, Paul Langerhans Institute Dresden of the Helmholtz Center Munich at University Hospital Carl Gustav Carus, Technische Universität Dresden, Fetscherstraße 74, 01307 Dresden, Germany; [6]Institut Kardiale Diagnostik und Therapie (IKDT), Moltkestraße 31, 12203 Berlin, Germany; [7]Institute of Veterinary Pathology, Freie Universität Berlin, Kaiserswerther Str. 16-18, 14195 Berlin, Germany; [8]Department of Cardiology, Charité—Universitätsmedizin Berlin, Campus Virchow Klinikum (CVK), Charitéplatz 1, 10117 Berlin, Germany; [9]Department of Medicine III, University of Heidelberg, 69120 Heidelberg, Germany; DZHK (German Centre for Cardiovascular Research), Partner Site Heidelberg/Mannheim, University of Heidelberg, 69120 Heidelberg, Germany; [10]Medical Biotechnology Research Department, Genetic Engineering and Biotechnology Research Institute (GEBRI), City of Scientific Research and Technological Applications, Alexandria, Egypt and [11]Cardiopathology, Institute for Pathology and Neuropathology, University Hospital Tuebingen, Liebermeisterstr. 8, 72076 Tübingen, Germany

Received 13 March 2019; revised 29 August 2019; editorial decision 23 September 2019; accepted 4 October 2019

Time for primary review: 24 days

Aims The coxsackievirus B3 (CVB3) mouse myocarditis model is the standard model for investigation of virus-induced myocarditis but the pancreas, rather than the heart, is the most susceptible organ in mouse. The aim of this study was to develop a CVB3 mouse myocarditis model in which animals develop myocarditis while attenuating viral infection of the pancreas and the development of severe pancreatitis.

Methods and results We developed the recombinant CVB3 variant H3N-375TS by inserting target sites (TS) of miR-375, which is specifically expressed in the pancreas, into the 3′UTR of the genome of the pancreo- and cardiotropic CVB3 variant H3. *In vitro* evaluation showed that H3N-375TS was suppressed in pancreatic miR-375-expressing EndoC-βH1 cells >5 $\log_{10}$, whereas its replication was not suppressed in isolated primary embryonic mouse cardiomyocytes. *In vivo,* intraperitoneal (i.p.) administration of H3N-375TS to NMRI mice did not result in pancreatic or cardiac infection. In contrast, intravenous (i.v.) administration of H3N-375TS to NMRI and Balb/C mice resulted in myocardial infection and acute and chronic myocarditis, whereas the virus was not detected in the pancreas and the pancreatic tissue was not damaged. Acute myocarditis was characterized by myocardial injury, inflammation with mononuclear cells, induction of proinflammatory cytokines, and detection of replicating H3N-375TS in the heart. Mice with chronic myocarditis showed myocardial fibrosis and persistence of H3N-375TS genomic RNA but no replicating virus in the heart. Moreover, H3N-375TS infected mice showed distinctly less suffering compared with mice that developed pancreatitis and myocarditis after i.p. or i.v application of control virus.

Conclusion In this study, we demonstrate that by use of the miR-375-sensitive CVB3 variant H3N-375TS, CVB3 myocarditis can be established without the animals developing severe systemic infection and pancreatitis. As the H3N-375TS myocarditis model depends on pancreas-attenuated H3N-375TS, it can easily be used in different mouse strains and for various applications.

* Corresponding author. Tel: +49 30 31 47 21 81; fax: +49 30 31 42 75 02, E-mail: henry.fechner@tu-berlin.de

† These authors contributed equally to this work.

Keywords CoxsackievirusB3 • Pancreatitis • Myocarditis • Mouse model • Intravenous • Intraperitoneal • Inflammation • Virus • Heart • Pancreas • icroRNA target sites

1. Introduction

Coxsackieviruses of group B (CVB) are non-enveloped, single-(+) stranded RNA viruses, which belong to the genus *Enterovirus* of the family *Picornaviridae*. Systemic infection with CVB occurs via the gastrointestinal tract. After entering via the small intestine, the virus infects adjacent organs and later spreads to other organs.[1] Acute CVB infection can cause mild (flu-like symptoms) to severe (aseptic meningitis, encephalitis, and myocarditis) disease. In newborns, CVB can induce severe systemic infection, leading to cardiac or multi-organ failure.[2,3] In adults, cardiac CVB infection is of particular importance.[4] CVB is found in almost 25% of patients with viral myocarditis and CVB3 is the most studied human pathogen of viral myocarditis.[5] In the heart, CVB infects not only cardiomyocytes but also endothelial cells, cardiac fibroblasts, and immune cells[3,6,7] leading to induction of acute, subacute, and chronic myocarditis. The acute form is characterized by detection of virus in the heart, damage of cardiomyocytes, and infiltration of the tissue with immune cells. Acute myocarditis can resolve or proceed to chronic myocarditis.[8,9] This stage is associated with persistence of the CVB genome and persistent inflammation and progressive fibrosis in the absence of replicating virus.[8,10] As a consequence of disease progression, patients can develop severe cardiac dysfunction, dilated cardiomyopathy, and heart failure.[11,12]

A mouse model of experimental CVB-induced myocarditis was established about 60 years ago by intraperitoneal (i.p.) infection of mice with CVB3.[13,14] Because of the resemblance of myocardial injury in mice to that occurring naturally in humans[15,16] this model has become the standard for the investigation of experimentally virus-induced myocarditis *in vivo*. Infection of mice with CVB3 typically results in multi-organ disease, often with a fatal outcome.[1,17] The pancreas is the most susceptible organs for CVB3 in mice[4,18,19] and infection of the pancreas seems to be of particular importance for development of murine myocarditis. Frequently, it has been assumed that the pancreas is the first major site of abundant virus replication, acting as a reservoir from which the virus spreads to the heart and probably determines the cardiovirulence of the virus.[1,18,20,21] However, the latter has not been definitively clarified yet, as a more recent study concluded that pancreatic infection has little effect on cardiac CVB3 infection and pathology.[22]

According to the course of infection, the CVB3 mouse myocarditis model mimics CVB3 disease in infants rather than in adults.[18] In particular, severe systemic disease and severe pancreatitis, which almost always occurs in infected mice,[18] is a rare event in adult patients with myocarditis.[23] In this study, we analysed the possibility of restricting CVB3 infection to the heart, while attenuating its replication in the pancreas. To this end, we developed the genetically engineered CVB3 variant H3N-375TS bearing target sites (TS) to the pancreas-specific expressed miR-375. The virus was studied for its sensitivity to miR-375, and for its replication in cardiac and pancreatic cells *in vitro*. Furthermore, H3N-375TS was evaluated for its ability to induce myocarditis and pancreatitis *in vivo* in two mouse strains.

2. Methods

An expanded Methods section is available in the Supplementary material online.

2.1 Development of recombinant miR-TS-containing CVB3, determination of virus concentration and titration

For cloning and engineering of recombinant CVB3 bearing miR-TS, the plasmid pBKCMV-H3 containing cDNAs of the genome of pancreotropic and cardiotropic CVB3 strain H3[24] was used. Viruses were propagated by transfection of CVB3 cDNA plasmids into HEK293T cells and amplified in HeLa cells. Virus for intravenous (i.v.) application was purified and concentrated by ultracentrifugation through a 30% sucrose solution before use. To determine viral titres, viral plaque assays were conducted as previously described.[25]

2.2 Cell cultures

HEK293T cells, HeLa cells and the pancreatic cell lines EndoC-βH1, PANC-1, and INS-1E were used for the *in vitro* investigations. Embryonic mouse cardiomyocytes (EMCMs) were obtained from C57BL/6 mice on embryonic day 14 and cultured as described elsewhere.[26]

2.3 MiR microarrays, quantification by RT–PCR

MiR microarrays were conducted with Affymetrix GeneChip miRNA 3.0 microarrays (Affymetrix Inc., Santa Clara, CA, USA). Expression levels of pro-inflammatory cytokines IL-6, IL-2, IL-1β, IFNγ, and TNF-α and microRNAs (miRs) were determined utilizing specific FAM-tagged TaqMan gene expression assays from Life Technologies (Waltham, MA, USA). For quantification of viral RNA, real-time PCR was performed using the primers 5′-CCCTGAATGCGGCTAATCC-3′ and 5′-ATTGTC ACCATAAGCAGCCA-3′ and Sso Fast™ EvaGreen Supermix (Bio-Rad, Hercules, CA, USA).

2.4 Western blot analysis, luciferase reporter assay, immunohistochemistry, and laser micro-dissection

Western blot analysis for detection of VP1 and γ-tubulin was carried out as described.[27,28] *Firefly* and *Renilla* luciferase activities were measured using the Dual-Luciferase Reporter Assay (Promega GmbH, Mannheim, Germany). Immunostaining, image acquisition, and processing were performed as described.[27] Laser micro-dissection of pancreas tissue was carried out as described.[29]

2.5 Plasmid and miR-Mimics transfection

HEK293T cells were seeded in six well plates and 24 h later, at a confluence of 70–90%, they were transfected with plasmid-DNA using Polyethylenimine MAX 40K (Polysciences, Warrington, PA, USA). HeLa cells were transfected with miR-mimics using RNAi Max (Life Technologies) as transfection reagent.

2.6 *In vivo* CVB3 infection

To investigate the acute course of CVB3 infection following i.p. application, 6-week-old female NMRI mice (Charles River, Sulzfeld, Germany) were i.p. infected with 1×10^5 plaque forming units (pfu) of virus. To investigate the acute course of CVB3 infection following i.v. application, 6-week-old female NMRI and female Balb/C mice (Charles River) were

anaesthetized with isofluran and 5×10^4 to 1×10^8 pfu of virus were injected into the left jugular vein. All animals were analysed 7 days after virus infection, and Balb/C mice were also analysed 3 days after infection. To investigate the chronic course of CVB3 infection, the virus was applied i.v. to NMRI mice as described above. Animals were sacrificed by cervical dislocation and analysed 28 days after viral infection. All *in vivo* procedures were performed in accordance with the European principles of laboratory animal care (Directive 2010/63/EU) and approved by the local ethics committee (Landesamt für Gesundheit und Soziales, Berlin, Germany).

2.7 Physical condition score, histopathological analysis, and haemodynamic measurements

The physical condition was scored by assessment of activity and body posture by clinical inspection. For histopathological analyses, mouse tissues were fixed in 4% formalin, embedded in paraffin, and 5 µm cross-sections were cut and stained with haematoxylin and eosin (H&E) or with Masson's trichrome to visualize fibrosis. To quantify myocardial damage comprising cardiac cell necrosis, inflammation and scarring, a myocarditis score was applied as described.[30] Haemodynamic measurements of cardiac function were recorded via conductance catheter in an open-chest model as described previously.[31]

2.8 Statistics

Results are expressed as means ± SEM. To test for statistical significance of *in vitro* data, an unpaired Student's *t*-test was applied. Statistical significance of *in vivo* data was determined using the Mann–Whitney *U* test.

3. Results

3.1 Evaluation of a pancreas-specific expressed miR

To achieve selective inhibition of replication of a miR-TS containing CVB3 in the murine pancreas, it was necessary to identify a miR which is highly expressed in the pancreas with negligible expression in the heart. Utilizing miR-chip analysis, we initially selected nine miRs (miR-690, miR-375, miR-217, miR-216a, miR-216b, miR-200a, miR-200b, and miR-200c) for further analysis because of their high expression in the murine pancreas (results not shown). Quantitative (q)RT–PCR revealed that miR-375 and miR-690 were the most highly expressed in the pancreas. In the heart, however, all miRs were barely expressed, with exception of miR-690 which was distinctly expressed (*Figure 1A*). Therefore, the most highly and selectively expressed miR in the pancreas, miR-375, was selected for further analysis of its expression in the exocrine pancreas. This tissue represents the primary site of CVB3 replication in the murine pancreas (25). Using laser micro-dissection of pancreatic tissue and qRT–PCR, we confirmed high expression of miR-375 in the exocrine pancreas (*Figure 1B*). Finally, we analysed whether miR-375 recognizes miR-375TS. To this end, three copies of the miR-375TS with perfect complementarity to the mature miR-375 were inserted into the 3′UTR of a luciferase expression cassette. Following co-transfection of the resulting luciferase reporter plasmid with a miR-375 expression plasmid, a strong silencing of luciferase expression was detected, confirming interaction of miR-375 with miR-375TS (*Figure 1C*).

3.2 H3N-375TS is efficiently inhibited in miR-375TS expressing pancreatic EndoC-βH1 cells but not in primary EMCMs

Previously we have shown that efficient gene silencing can be achieved by insertion of three copies of a miR-TS into the 3′UTR of a gene expression cassette.[32] Thus, here three copies of the miR-375TS were inserted into the 3′UTR of the RNA genome of the pancreo- and cardiotropic CVB3 strain H3, leading to generation of H3N-375TS. A control virus (H3N-39TS) was generated by insertion of three copies of a miR-TS of the non-mammalian cel-miR-39 into the 3′UTR of the H3 genome (*Figure 2A*).

To elucidate whether H3N-375TS can be inhibited by miR-375, we transfected HeLa cells with miR-375 mimics or miR control mimics and infected the cells with H3N-375TS, H3N-39TS, or with H3. Plaque assay carried out 24 h later revealed that H3N-375TS progeny production was strongly inhibited by about 63-fold (98.6%) by miR-375TS mimics, whereas they did not affect replication of H3N-39TS and H3 (*Figure 2B*). To confirm that H3N-375TS replication is also inhibited in pancreatic cells with endogenously expressed miR-375, three pancreatic cell lines (Panc-1, INS-E1, and EndoC-βH1) were investigated for their miR-375 expression and their susceptibility to CVB3. Only EndoC-βH1 expressed high amounts of miR-375 and was susceptible to CVB3 (Supplementary material online, *Figure S1A–C*). Therefore, this cell line was used in all further investigations. Following infection of EndoC-βH1 with H3N-375TS, replication of the virus was strongly inhibited by >5 orders of magnitude compared with H3N-39TS and H3, as determined by virus plaque assay (*Figure 2C*). Inhibition of H3N-375TS replication in EndoC-βH1 was confirmed by determination of expression of the H3N-375TS VP1 and cleavage of the eukaryotic translation initiation factor eIF4G using western blots. Neither VP-1 expression nor cleavage of eIF4G was found in H3N-375TS-infected EndoC-βH1 cells, whereas H3N-39TS and H3 infected cells showed abundant VP1 expression and cleavage of eIF4G (*Figure 2D*). To confirm uninhibited replication of H3N-375TS in cardiac cells, EMCMs were infected with H3N-375TS and analysed by plaque assay for production of viral progeny. The H3N-375TS titres were very similar to those of the control viruses H3N-39TS and H3, demonstrating that the replication of H3N-375TS was uninhibited in cardiac cells (*Figure 2E*).

3.3 Intraperitoneal-injected H3N-375TS does not induce pancreatitis and myocarditis in NMRI mice

Intraperitoneal inoculation of adult mice with H3 leads to severe disease with pancreatic and myocardial CVB3 infection.[19,21] To prove that H3N-375TS does not replicate in the pancreas but infects the heart, we infected NMRI mice i.p. with 1×10^5 pfu of H3N-375TS or the control virus, H3N-39TS. The mice were analysed 7 days later, when acute myocarditis occurs after CVB3 infection.[21] As the clinical parameters to assess the severity of CVB3 disease, we determined body weight development and assigned a physical condition score. The body weight of H3N-375TS infected mice was unchanged, whereas the physical condition score was slightly reduced when compared to uninfected mice. In contrast, both parameters were distinctly reduced in H3N-39TS infected control animals (*Figure 3A*). Virus titres in the heart were determined by virus plaque assay, whereas qRT–PCR was used to determine virus titres in the pancreas. Correlating with the reduced physical

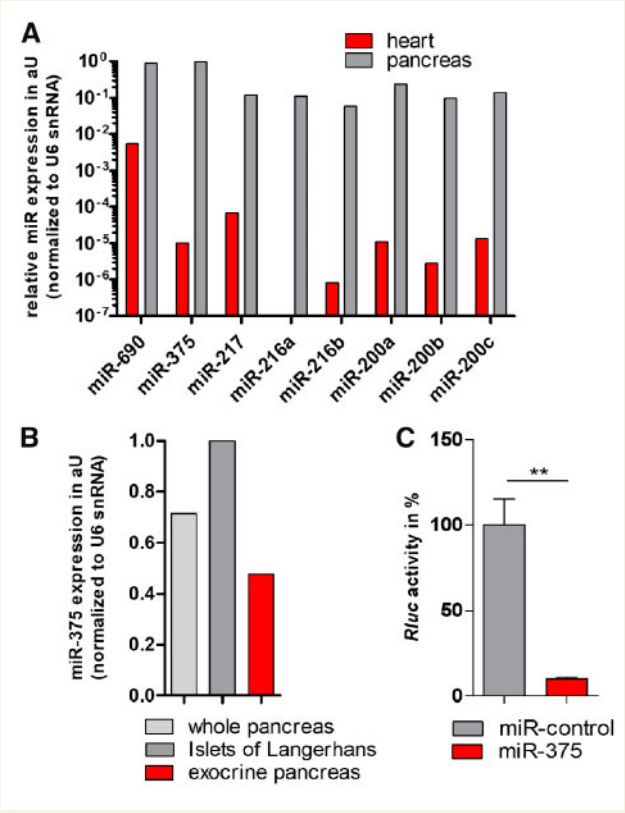

Figure 1 Expression of miRs in the pancreas and heart of mice *in vivo* and *in vitro* silencing of miR-375TS-bearing luciferase reporter by miR-375. (*A*) Expression levels of miRs in the pancreas and heart of mice. Expression of the miRs was determined by qRT–PCR and normalized against U6 snRNA; aU, arbitrary units. (*B*) Expression of miR-375 in the whole pancreas, the exocrine pancreas, and in the Islets of Langerhans of mice. Exocrine pancreas and Islets of Langerhans were dissected by laser micro-dissection from murine pancreas tissue and investigated for miR-375 expression by qRT–PCR. Expression levels in both tissues are shown relative to whole pancreas (set = 1). Expression of the miRs was normalized against U6 snRNA. (*C*) Silencing of miR-375TS-bearing firefly luciferase reporter by miR-375. HeLa cells were transfected with miR-375 expression plasmid pCMV-MIR-375-GFP (miR-375) or control plasmid pscAAV-amiR-Hex (miR control) expressing an artificial miR directed against the hexon gene of adenovirus 5. Cells were co-transfected with pLuc-miR-375TS containing a miR-375TS in the 3′UTR of a *Renilla* luciferase (*Rluc*) reporter and luciferase activity was determined 48 h later. *Rluc* activity was normalized against activity of firefly luciferase, which was co-expressed from the same reporter plasmid. Silencing of miR-375TS bearing reporter was calculated relative to control (set = 100%). Statistical significance was determined using unpaired Student's *t*-test; $^{**}P < 0.01$. The experiment was performed twice, each time in duplicate.

condition, H3N-39TS was detected at high titres of 5.8×10^3 copies/µg RNA and 1.5×10^6 pfu/g tissue in the pancreas and the heart, respectively (*Figure 3B*), and animals developed acute pancreatitis with massive destruction of the exocrine pancreas tissue and moderate myocarditis (myocarditis score 1.3) with multifocal tissue destruction and infiltration of mononuclear cells (*Figure 3C, D*). In contrast, H3N-375TS was only detected in the pancreas and the heart of two of seven animals, but even in these cases at very low levels (*Figure 3B*). Correlating with the lack of pancreatic and cardiac infection, the pancreas and heart tissues of H3N-375TS-infected animals were intact and neither necrosis nor inflammation was seen (*Figure 3C, D*).

3.4 Intravenous-injected H3N-375TS causes no pancreatitis but pronounced acute myocarditis in NMRI mice

Based on the above results, we assumed that i.p. inoculation of H3N-375TS leads to infection of the pancreas, where avoidance of viral replication by miR-375 subsequently prevents viraemia and cardiac infection with H3N-375TS. Thus, we directly inoculated 5×10^4 to 5×10^6 pfu of H3N-375TS via the jugular vein into the blood stream and investigated animals 7 days later. Indeed, mice exhibited cardiac infection, accompanied by cardial injury and inflammatory cell infiltration, whereas the pancreas remained uninfected. However, even at the highest dose used the cardiac titres (1.5×10^3 pfu/g) and the myocarditis scores (0.75) were rather low (Supplementary material online, *Figure S2*). To investigate whether H3N-375TS-induced myocarditis can be made more severe, we repeated the experiment and injected NMRI mice with 5×10^6 pfu of H3N-375TS, which was isolated from NMRI mice showing the highest virus titre in the heart in the previous experiment. Heart passaging (*hp*) can increase the cardiovirulence of CVB3, whereas it does not attenuate pancreatic infection.[32] Alternatively, animals were infected with high dose (1×10^8 pfu) of H3N-375TS. H3N-39TS at a dose of 5×10^6 pfu per animal was used as a control. Even though body weight development in H3N-39TS infected mice was similar to that of uninfected control mice, H3N-39TS infection led to obvious suffering of the animals, as shown by a distinctly reduced physical condition score (*Figure 4A*). Both the pancreas and the heart were infected with H3N-39TS (*Figure 4B*), leading to severe acute pancreatitis and moderate myocarditis (*Figure 4C, D*). In contrast, mice infected with *hp* and high-dosed H3N-375TS showed an only slightly reduced physical condition score (*Figure 4A*). Virus was not detected in the pancreas and there was no destruction of the pancreas (*Figure 4B–D*). Importantly, cardiac virus titres reached 2.6×10^4 pfu/g and 1.36×10^4 pfu/g for the *hp* and high-dosed H3N-375TS, respectively (*Figure 4B*), which was higher than in the previous experiment and in the range of virus titres measured in the H3N-39TS-infected control mice. Moreover, the cardiac myocarditis scores were also higher, with values of 1.75 and 1.4 (*Figure 4C, D*), compared with the previous experiment but similar to those of H3N-39TS control animals. We also found an increase in cardiac expression of proinflammatory cytokines TNFα, IFNγ, and IL-6 (Supplementary material online, *Figure S3*), which are known to be induced in the hearts of mice with cardiac CVB3 infection,[33] when we compared animals infected with 1×10^8 pfu H3N-375TS to mock-infected mice.

3.5 Intravenous-injected H3N-375TS induces myocarditis but no pancreatitis in Balb/C mice

To find out whether H3N-375TS induces a similar course of infection in a more susceptible mouse strain,[20] we next investigated Balb/C mice for infection with H3N-375TS. Balb/C mice were infected i.v. with H3N-375TS at a dose of 5×10^6 or 1×10^8 pfu per animal or with the control virus H3N-39TS at 5×10^6 pfu and investigated 7 days later. The H3N-375TS-infected mice showed body weight development and physical condition scores similar to the uninfected control mice, whereas both parameters were strongly reduced in the control group infected with H3N-39TS (Fig. *5A*, Supplementary material online, *Video S1–S3*).

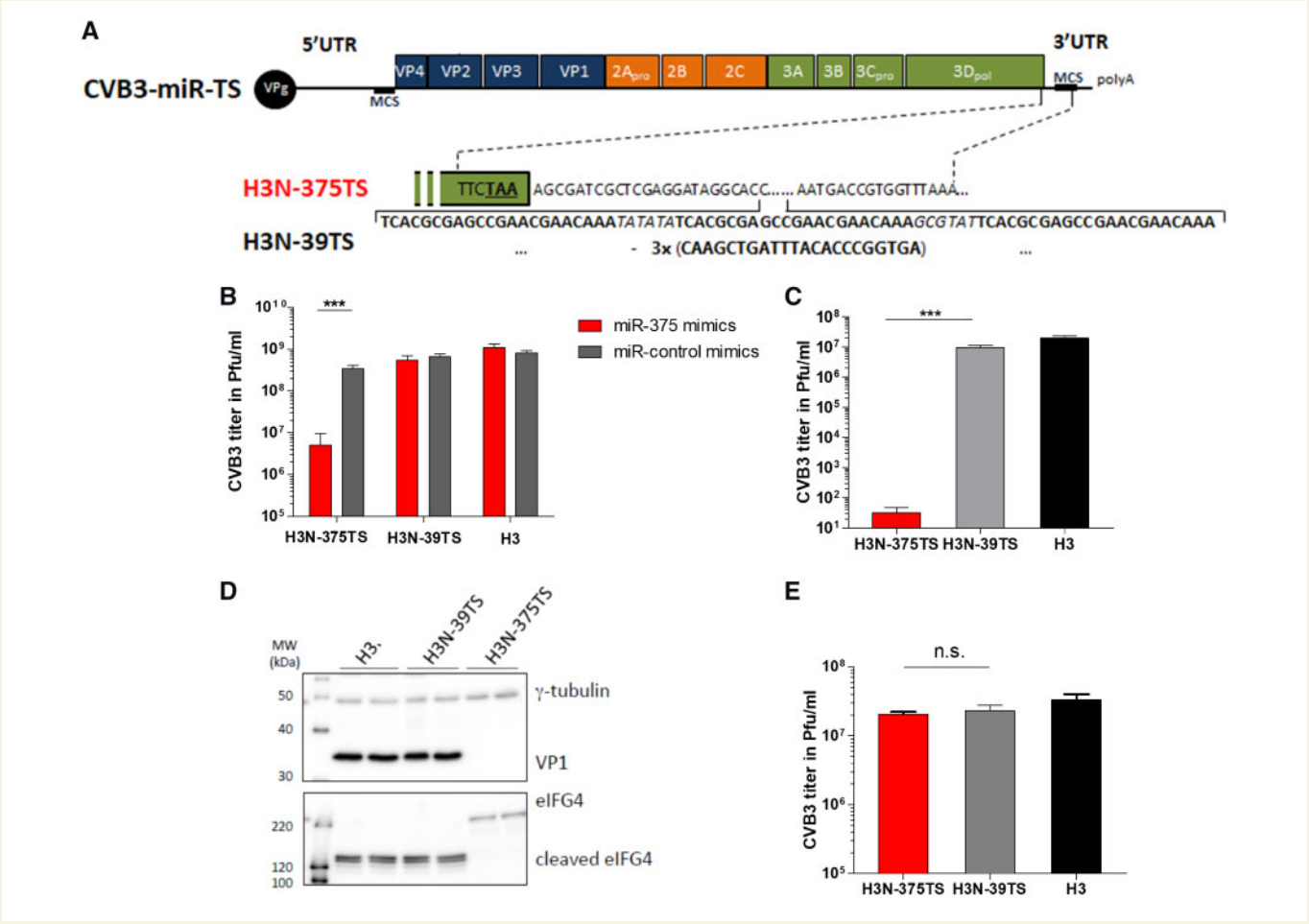

Figure 2 H3N-375TS is suppressed in pancreatic but not cardiac cells *in vitro*. (*A*) Genomic structure of H3N-375TS and H3N-39TS. Three copies of the miR-375TS or the miR-39TS were inserted immediately downstream of the stop codon of the CVB3 polyprotein in the 3′UTR of the viral genome of the CVB3 strain H3. Bold letters show the respective miR-TS. Letters in italics represent spacer sequences, which separate the miR-TS. (*B*) Inhibition of H3N-375TS by miR-375TS mimics. HeLa cells were transfected with 50 nM miR-375 mimics or control miR-mimics and infected 4 h later at an MOI of 0.1 with H3N-375TS, H3N-39TS, or H3. After 24 h, virus was harvested and plaque assays carried out to determine CVB3 titres. The data are shown for each animal and as mean values ±SEM for each group. (*C*) Inhibition of H3N-375TS replication in pancreatic EndoC-βH1 cells. EndoC-βH1 cells were infected with H3N-375TS, H3N-39TS, and H3, each with a low MOI of 0.0002, as EndoC-βH1 cells are highly sensitive to H3. Virus replication was analysed 24 h later by plaque assay. (*D*) Inhibition of VP1 expression and cleavage of the eukaryotic translation initiation factor eIF4G in H3N-375TS-infected EndoC-βH1 cells. Cells were infected with H3N-375TS, H3N-39TS, or H3, each at an MOI of 0.0002. Expression of VP1 and eIF4G was analysed 48 h later by western blot. The internal loading control was γ-tubulin. (*E*) H3N-375TS is not suppressed in EMCMs. EMCMs were infected at an MOI of 0.1 with H3N-375TS, H3N-39TS, or H3. Virus replication was determined 48 h later by plaque assay. The experiments (*B–E*) were performed twice, each time in duplicate. Statistical significance in (*B*), (*C*), and (*E*) was determined using unpaired Student's *t*-test; ***$P < 0.001$; n.s., not significant.

The pancreas of the H3N-375TS-infected animals was virus-free and the pancreatic tissue was intact (*Figure 5B–D*). The cardiac virus titres were very similar in both H3N-375TS-infected animal groups, measured at 8.6×10^3 pfu/g for the low and 5.2×10^3 pfu/g for the high-dose H3N-375TS, but they were significantly lower than the 1.2×10^5 pfu/g measured in the H3N-39TS-infected animals (*Figure 5B*). The cardiac myocarditis score was similar in both H3N-375TS groups, with scores of 1.7 and 2.0, which is very similar to the 1.8 seen for the H3N-39TS-infected animals (*Figure 5C, D*). We also carried out haemodynamic measurements to determine cardiac function. Whereas H3N-39TS-infected mice showed impaired left ventricular cardiac function, the cardiac function of mice infected with H3N-375TS was similar to that of uninfected control mice (Supplementary material online, *Table S1*). To elucidate whether the lack of cardiac dysfunction in H3N-375TS-infected mice results from less cardiac injury or is related to a specific inflammatory process, we infected Balb/C mice with 1×10^8 pfu H3N-375TS or with 5×10^6 pfu H3N-39TS and measured the serum levels of cardiac troponin T (hcTnT) and determined IFNγ, TNFα, IL-6, IL-1β, and IL-2 levels in the heart and the pancreas 3 days later. Whereas both animal groups showed high and similar hcTnT serum levels, which correlated with similar cardiac virus titres (*Figure 6A*), the cytokines were differentially expressed. In the heart, all cytokines were induced in both animal groups but higher levels were found for IFNγ and IL-2 in H3N-375TS-infected mice (*Figure 6D*). In the pancreas, which was damaged by H3N-39TS but not by H3N-375TS (*Figure 6B, C*) only IFNγ and IL-1β were detected in H3N-375TS-infected mice but remained at very low levels. In contrast,

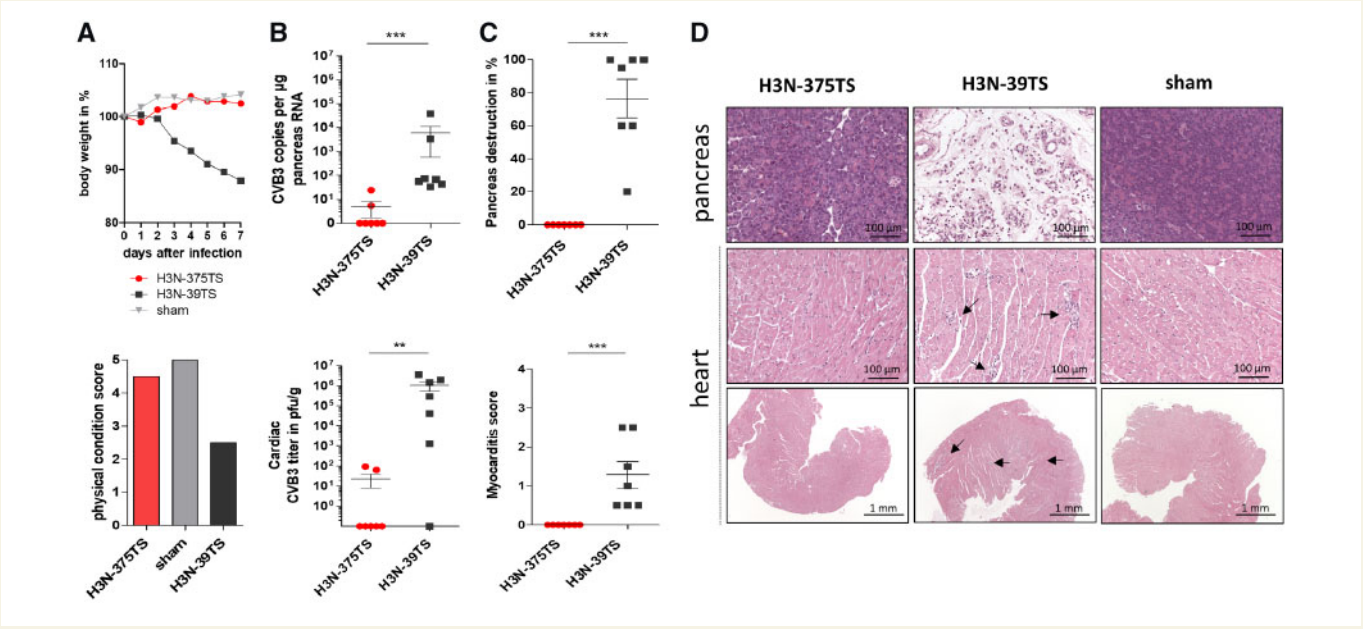

Figure 3 Intraperitoneal injection of H3N-375TS in mice does not lead to pancreatic and myocardial infection. NMRI mice were infected i.p. with 1×10^5 pfu of H3N-375TS ($n = 7$) or H3N-39TS ($n = 7$) or were mock-infected ($n = 7$). Animals were sacrificed 7 days later and analysed. (*A*) Body weight development and physical condition. *Upper diagram:* Body weight development. *Lower diagram*: Physical condition score. Physical condition was determined for each animal and quantified by a scoring system ranging from 1 (low) to 5 (high). (*B*) Viral titres in the pancreas and the heart. *Upper diagram:* The number of CVB3 genome copies in the pancreas was determined by qRT–PCR. *Lower diagram*: The amount of infectious CVB3 in the heart was determined by plaque assay. (*C*) Pathological alterations of the pancreas and the heart. *Upper diagram*: Pancreas sections were stained with H&E and tissue injury was quantified by a scoring system from 0 (no tissue alteration) to 100% (complete organ destruction). *Lower diagram:* Heart sections were stained with H&E and the degree of myocarditis was quantified by a scoring system ranging from 0 (none) to 4 (high). (*D*) Shown are representatives of H&E stained formalin-fixed pancreas and heart slides. Arrows indicate tissue areas with infiltration of inflammatory cells. (*A*) Shown are mean values of a group of animals; (*B*, *C*) Data are shown for each animal and as mean values ± SEM for each group. Note: mock-infected animals had no alterations of the pancreas and heart tissue and virus was not detected in either tissue (not shown). Statistical significance in (*B*) and (*C*) was determined using the Mann–Whitney *U* test.; $^{**}P < 0.01$, $^{***}P < 0.001$.

H3N-39TS-infected mice showed very strong expression of IFNγ, TNFα, IL-6, and IL-1β (*Figure 6D*).

3.6 NMRI mice intravenously infected with H3N-375TS develop chronic myocarditis but not pancreatitis

NMRI mice develop chronic myocarditis after i.p. infection with the CVB3 strain H3.[21] To prove that H3N-375TS can also induce chronic myocarditis, we infected NMRI mice i.v. with 1×10^8 pfu of *hp* H3N-375TS and investigated the animals 28 days later. Body weight of the mice decreased markedly within the first 2 days after infection and two animals died 2 days after virus injection. The others recovered and after day 7 body weights of H3N-375TS-infected animals developed as in the non-infected control mice (*Figure 7A*). The physical condition score analysed at day 28 did not differ between infected and uninfected control animals (results not shown). Histological examinations showed no alteration of pancreatic tissue (*Figure 7B*) and there was no virus detected in the pancreas of H3N-375TS-infected animals (results not shown). In contrast, heart tissue revealed increased collagen deposition in areas of the cardiac lesion, as determined by trichrome staining (*Figure 7B*) and persistence of H3N-375TS genomic RNA (*Figure 7C*), whereas replicating virus was not detected in the heart (results not shown). The myocarditis score was 1, demonstrating that the majority of H3N-375TS-infected animals developed mild chronic myocarditis (*Figure 7D*). We also determined the LV cardiac function by measurement of haemodynamics at the end of the investigational period. No differences in LV cardiac function between H3N-375TS infected and uninfected NMRI mice were found (Supplementary material online, *Table S2*).

4. Discussion

In the classical CVB3 mouse myocarditis model infection with CVB3 results in severe systemic disease with the pancreas as the organ most susceptible to injury. Therefore, this model most closely mimics the course of systemic multi-organ disease found in infants, as has already been stated years ago by Tracy *et al.*,[18] rather than the course of CVB3 disease in adult patients where viral myocarditis is paramount.[4] Here, we report on a new CVB3 myocarditis model in which, after i.v. application of the genetically engineered miR-375-sensitive CVB3, termed H3N-375TS, infected mice develop acute and chronic myocarditis but do not develop severe systemic disease and pancreatitis.

Previous studies of Tracy *et al.*[18] and Horwitz *et al.*[1] found evidence that in mice the heart cannot be infected with CVB3 when the pancreas is not infected. Both studies used i.p. application to infect the mice with CVB3. Using the same route of administration, here, we found that the pancreas-attenuated CVB3 variant H3N-375TS was unable to infect the heart, confirming that, following i.p. infection, virus replication in the pancreas is essential for cardiac infection and development of myocarditis.

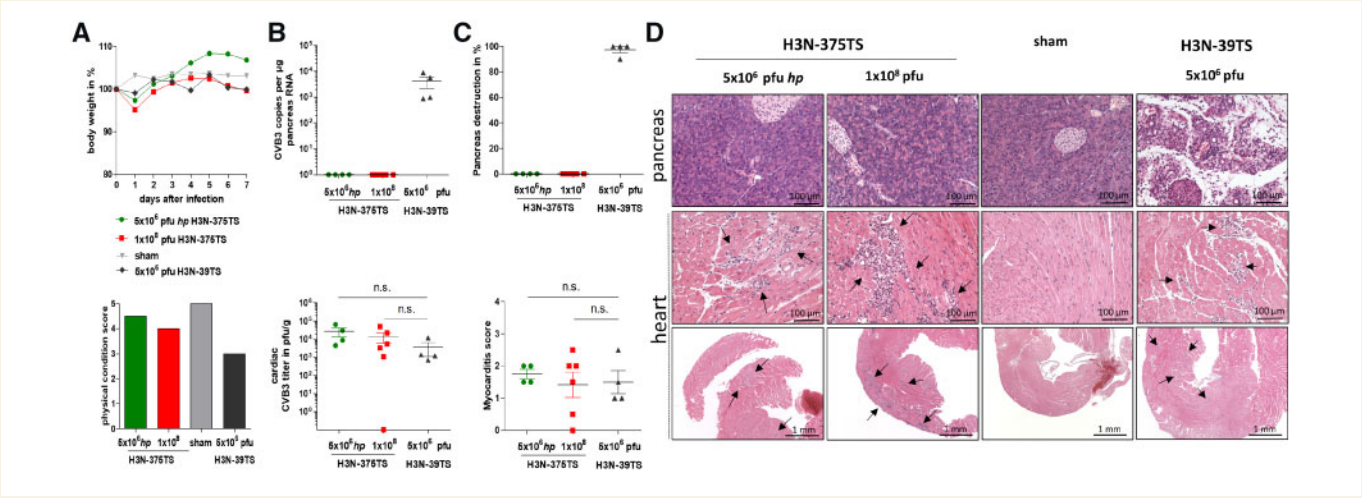

Figure 4 Intravenous injection of *hp* or high-dosed H3N-375TS results in development of moderate myocarditis but not pancreatitis in NMRI mice. Mice were infected i.v. with 5×10^6 pfu of *hp* H3N-375TS ($n = 4$) or high dose of 1×10^8 pfu of H3N-375TS ($n = 6$) or with 5×10^6 pfu of the control virus H3N-39TS ($n = 4$). A fourth group of mice was mock-infected (sham; $n = 6$). Animals were sacrificed at day 7 after infection and analysed. (*A*) Body weight development and physical condition. Body weight development (*upper diagram*) and physical condition score (*lower diagram*) were determined as in *Figure 3A*. (*B*) Virus titres in the pancreas and the heart. The number of CVB3 genome copies in the pancreas (*upper diagram*) and the amount of infectious CVB3 in the heart (*lower diagram*) were determined as in *Figure 3B*. (*C*) Pathological alterations of the pancreas and the heart. Pancreas destruction (*upper diagram*) and myocarditis score (*lower diagram*) were determined as in *Figure 3C*. (*D*) Shown are representatives of H&E stained formalin-fixed pancreas and heart slides. Arrows indicate tissue areas with infiltration of inflammatory cells. (*A*) Shown are mean values of a group of animals; (*B*, *C*) Data are shown for each animal and as mean values ± SEM for each group. Note: mock-infected animals had no alterations of pancreas and heart tissue and virus was not detected in either tissue (not shown). Statistical significance in (*B*) and (*C*) was determined using the Mann–Whitney *U* test; n.s., not significant.

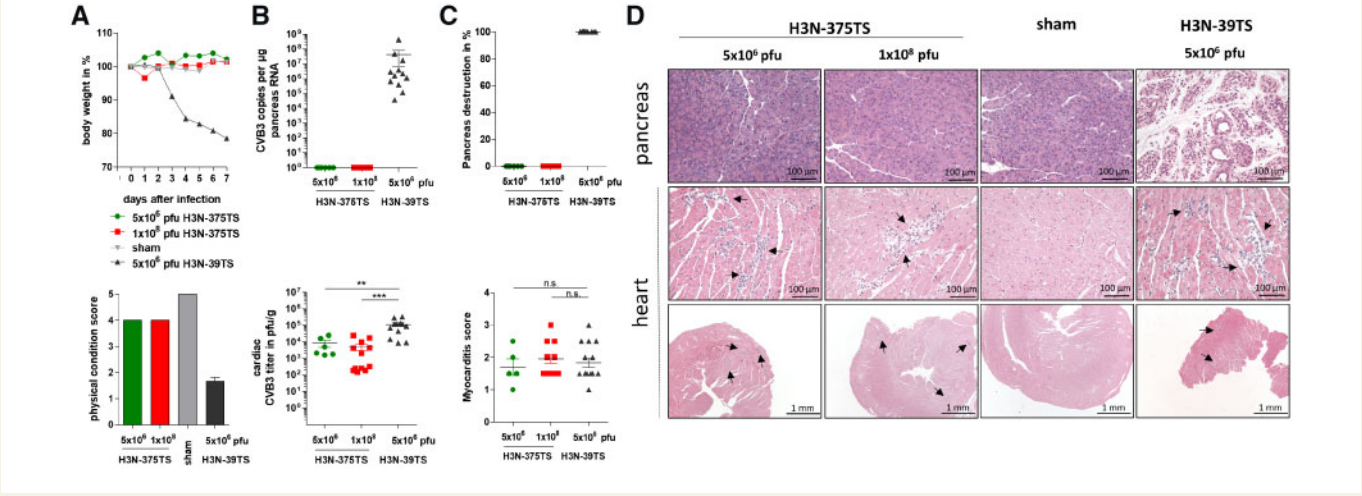

Figure 5 Intravenous injection of H3N-375TS results in moderate myocarditis but no pancreatitis in Balb/C mice. Mice were infected i.v. with 5×10^6 pfu of H3N-375TS ($n = 6$) or 1×10^8 pfu of H3N-375TS ($n = 12$), or with 5×10^6 pfu of the control virus H3N-39TS ($n = 12$). A fourth group contained mock-infected (sham; $n = 10$) animals. Animals were sacrificed and analysed at day 7 after infection. (*A*) Body weight development and physical condition. Weight development (*upper diagram*) and physical condition score (*lower diagram*) were determined as in *Figure 3A*. (*B*) Virus titres in the pancreas and the heart. The number of CVB3 genome copies in the pancreas (*upper diagram*) and the amount of infectious CVB3 in the heart (*lower diagram*) were determined as in *Figure 3B*. (*C*) Pathological alterations of the pancreas and the heart. Pancreas destruction (*upper diagram*) and myocarditis score (*lower diagram*) were determined as described in *Figure 3C*. (*D*) Representatives of H&E stained formalin-fixed pancreas and heart slides. Arrows indicate tissue areas with infiltration of inflammatory cells. (*A*) Shown are mean values of a group of animals; (*B*, *C*) Data are shown for each animal and as mean values ±SEM for each group. Statistical significance in (*B*) and (*C*) was determined using the Mann–Whitney *U* test; $^*P < 0.05$; $^{**}P < 0.01$. Note: Myocarditis score of one animal from the group infected with 5×10^6 pfu H3N-375TS could not be determined because of insufficient formalin fixation of heart tissue.

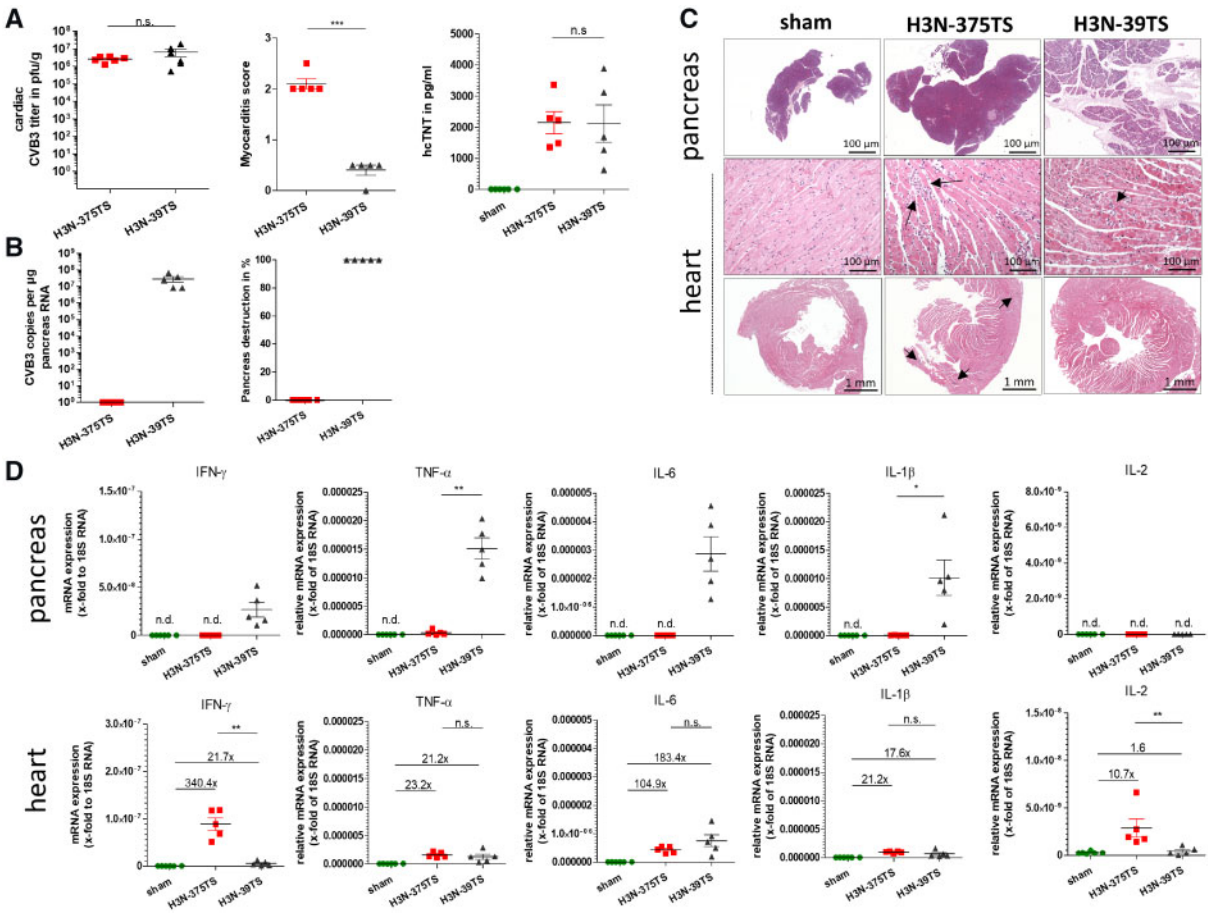

Figure 6 Intravenous injection of H3N-375TS and H3N-39TS induces similar cardiac injury but different cytokine profile in the pancreas and the heart. Mice were infected i.v. with 1×10^8 pfu of H3N-375TS ($n = 5$) or 5×10^6 pfu of the control virus H3N-39TS ($n = 5$) or were mock infected (sham; $n = 6$). Animals were sacrificed and analysed at day 3 after infection. (*A*) Virus titres, myocarditis scores, and hsTnT levels in the heart. The cardiac virus titres and the myocarditis score were determined as described in *Figure 3B, C*. Expression of hsTnT was measured by ELISA. (*B*) Viral titres in the pancreas and pancreas destruction. The number of CVB3 genome copies in the pancreas and pancreas destruction was determined as in *Figure 3B, C*. (*C*) Shown are representatives of H&E stained formalin-fixed pancreas and heart slides. Arrows indicate tissue areas with infiltration of inflammatory cells. (*D*) Cytokine levels measured in the pancreas and the heart. Cytokine levels were measured by real-time RT–PCR. To compare absolute gene expression between different animal groups gene expression is plotted as mean ±SEM as x-fold to 18S RNAs. (*A*, *B*, *D*) Data are shown for each animal and as mean values ± SEM for each group. n.d., not detectable. Statistical significance was determined using the Mann–Whitney *U* test; $^*P < 0.05$; $^{**}P < 0.01$; $^{***}P < 0.001$; n.s., not significant.

However, this conclusion contradicts a more recent study of Kallewaard *et al.*,[22] who concluded from CVB3 infection experiments in mice with pancreas-specific knock out of the coxsackievirus and adenovirus receptor (CAR), that infection of the pancreas with CVB3 has little effect on cardiac CVB3 infection and pathology. In contrast to our study, where CVB3 replication was completely abolished in the pancreas, in the study of Kallewaard *et al.* CVB3 was still detectable in the CAR knock group after i.p. virus administration. Considering this fact, it suggests that even low CVB3 replication in the pancreas is sufficient to induce pronounced cardiac virus infection and that there is no direct linear correlation between CVB3 replication in the pancreas and CVB3 infection of the heart.

Mimicking the natural spread of CVB3 via the blood stream, i.v. administration of H3N-375TS resulted in infection of the heart and induction of myocarditis, but importantly, the virus was not detected in the pancreas and its tissues remained intact. This demonstrates that CVB3 can directly infect the heart, without having previously replicated in the pancreas. It also reveals i.v. application as the key for the establishment of experimental CVB3 myocarditis in mice when using a pancreas-attenuated CVB3 as H3N-375TS. H3N-375TS-induced myocarditis was very similar to myocarditis in the classical CVB3 myocarditis model. In fact, acute myocarditis was characterized by myocardial injury, inflammation by mononuclear cells, induction of proinflammatory cytokines and detection of replicating H3N-375TS in the heart, whereas chronically infected mice exhibited progressive fibrosis and occurrence of persistent viral RNA in the heart. Hence, our data indicate that the pathogenesis H3N-375TS-induced myocarditis is a result of intrinsic cardiac mechanisms that are related to infection and replication of the virus in the heart.

Despite the similarities in the pathological pattern of myocarditis, the H3N-375TS mouse myocarditis model has several specific differences compared with the classical CVB3 myocarditis model. At first, the H3N-375TS dose necessary to induce H3N-375TS myocarditis after i.v.

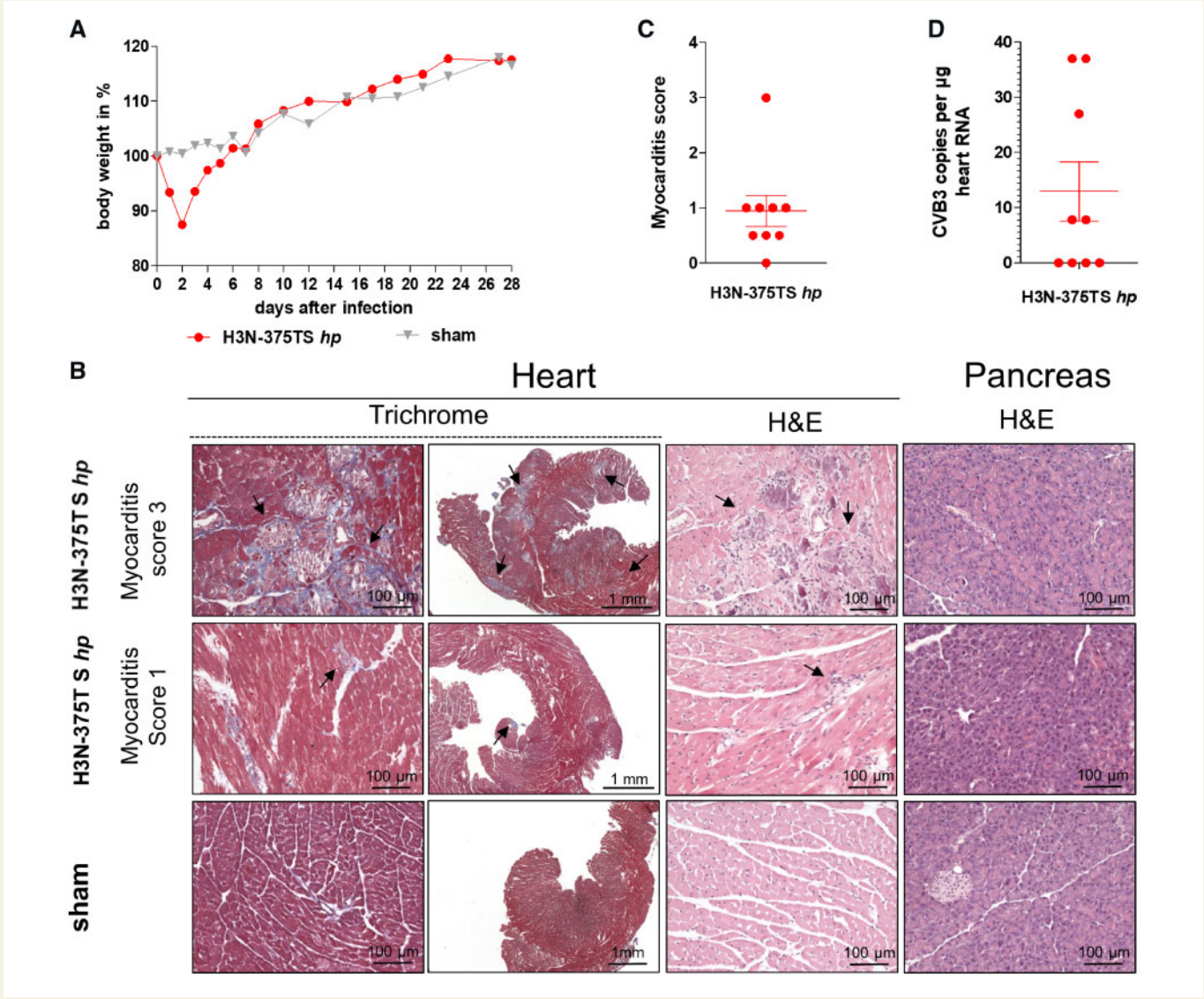

Figure 7 Intravenously applied *hp* H3N-375TS induces chronic myocarditis in NMRI mice. Mice were infected i.v. with 1×10^8 pfu of *hp* H3N-375TS ($n = 12$) or were mock-infected ($n = 11$, sham). Animals were sacrificed at day 28 after infection and analysed. (*A*) Body weight development. Shown are mean values of a group of animals. (*B*) Trichrome and H&E staining of formalin-fixed pancreas and heart slides of examples of each group. Arrows indicate tissue areas with infiltration of inflammatory cells. (*C*) Myocarditis score of H3N-375TS infected group. The score was determined as in *Figure 3B*. (*D*) Amount of H3N-375TS genomes in the heart. H3N-375TS genome copy number was determined by qRT–PCR. Note: mock-infected animals had no alterations of pancreas and heart tissue and virus was not detected in either tissue (not shown). Two animals infected with *hp* H3N-375TS died 2 days after infection. The myocarditis score and cardiac CVB3 RNA content were not determined for one animal of the group infected with *hp* H3N-375TS due to loss of the heart tissue during organ preparation.

injection is distinctly higher, whereas the cardiac virus titres are lower. Because of the very low expression of the miR-375 in the heart, we can rule out the possibility that the lower cardiac titres resulted from cardiac miR-375-mediated suppression of the H3N-375TS. Wild-type CVB3 infects the pancreas and replicates there over several days, leading to sustained high virus concentration in the blood and subsequent efficient infection of the heart.[6,18,24] In contrast, i.v. injected H3N-375TS circulates in the blood for only for short time. The latter may restrict efficient cardiac infection and lead to lower cardiac virus titres. We also observed that increasing the amount of injected H3N-375TS from 5×10^6 pfu to 1×10^8 pfu did not result in a further increase of cardiac H3N-375TS infection and inflammation scores. Even though the reason for this has yet not been elucidated, a limited capacity of cardiomyocytes to take up large amounts of CVB3 within a limited time may be a possible explanation. Hence, our data indicate that lack of pancreatic replication limits, but does not prevent, cardiac H3N-375TS infection.

As we have shown in previous studies, CVB3 myocarditis in mice can result in cardiac dysfunction.[31,33,34] Here surprisingly, neither Balb/C nor NMRI mice with H3N-375TS-induced acute and chronic myocarditis developed cardiac dysfunction. According to our current understanding, cardiac dysfunction in CVB3-infected mice is related to virus-induced damage of cardiomyocytes, cardiac inflammation, and cardiac remodelling. These parameters, however, were very similar in mice infected with H3N-375TS and in mice infected with the pancreotropic and

cardiotropic control virus H3N-39TS which induced cardiac dysfunction. It is conceivable that factors are released from extracardiac tissues as result of systemic CVB3 infection, which may contribute to development of cardiac dysfunction. We found that in the pancreas of H3N-39TS-infected mice several proinflammatory cytokines were strongly up-regulated, whereas they were not induced in the pancreas of H3N-375TS-infected mice. Among the cytokines are TNFα and IL-1β, which are known to contribute to myocardial dysfunction in an autocrine manner.[35,36] Considering that expression of both cytokines was distinctly stronger in the pancreas than in the heart of H3N-39TS-infected control mice, our data suggest that there may be a contribution of inflammatory processes in the virus-infected pancreas to functional alterations in the virus-infected heart. Lack of pancreatic inflammation in H3N-375TS-infected mice, however, would prevent this contribution, and may, therefore, be a possible explanation for the absence of cardiac dysfunction in H3N-375TS-infected mice.

Infection of mice with CVB3 results in severe sickness and can lead to the death of the animals.[1,17] Regarding this issue, it was an important finding of our study that H3N-375TS-infected mice showed distinctly better health status and body weight development than animals infected with H3N-39TS. The causal relationship between virus-induced pancreatitis and animal health status has not yet been definitively determined, but it has been suggested that degree of severity of virus-induced pancreatitis, probably in combination with additional strain specific factors, may contribute to health problems.[17,18] Our data support this conclusion. We only detected a transient impairment of health and death of 2 of 11 infected animals when we injected NMRI mice with *hp* H3N-375TS at a very high dose of 1×10^8 pfu. Infection with H3N-375TS that was not *hp* did not prove fatal to any of the infected mice, so this *hp* appears to be responsible for the observed adverse events.

In summary, here, we developed a new CVB3 myocarditis model by use of newly developed pancreas-attenuated H3N-375TS. We show that after i.v. application, H3N-375TS induces acute and chronic myocarditis in mice, whereas the animals do not develop pancreatitis. The use of H3N-375TS may allow the investigation of the pathogenesis of CVB3 myocarditis independently of severe systemic CVB3 disease and pancreatitis. Moreover, our study provides new insights into the pathogenesis of CVB3 myocarditis in mice, revealing the specific role of the pancreas and the virus application route for establishment of CVB3 myocarditis.

Supplementary material

Supplementary material is available at *Cardiovascular Research* online.

Acknowledgements

We gratefully thank Andreas Henke, Institute of Virology and Antiviral Therapy, Jena University Hospital, Friedrich Schiller University Jena, for providing the CVB3 cDNA clone H3 and Zhao-Hua Zhong, Department of Microbiology, Harbin Medical University, Harbin, China, for providing the plasmid pEGFP-CVB3. We thank Raphael Scharfmann, Institut Cochin, Université Paris Descartes, Paris, France for the provision of EndoC-βH1 cells. We also thank Erik Wade for critical reading of the manuscript and helpful comments.

Conflict of interest: none declared.

Funding

This work was supported by the Bundesministerium für Bildung und Forschung (*BMBF*) through grant 031A331 to S.P, C.T. and H.F. and through grant 2017.101.1 from the Wilhelm Sander-Stiftung to H.F and J.K.. Work in the Solimena lab is funded by the BMBF funded German Centre for Diabetes research (DZD e.V.). Additional funds for support of studies presented here came from the Innovative Medicines Initiative 2 Joint Undertaking (IMI2-JU) under grant agreement no. 115797 INNODIA. This joint undertaking receives support from the European Union's Horizon 2020 research and innovation programme and EFPIA, JDRF International and The Leona M. and Harry B. Helmsley Charitable Trust.

References

1. Horwitz MS, La Cava A, Fine C, Rodriguez E, Ilic A, Sarvetnick N. Pancreatic expression of interferon-gamma protects mice from lethal coxsackievirus B3 infection and subsequent myocarditis. *Nat Med* 2000;**6**:693–697.
2. Foulis AK, Farquharson MA, Cameron SO, McGill M, Schönke H, Kandolf R. A search for the presence of the enteroviral capsid protein VP1 in pancreases of patients with type 1 (insulin-dependent) diabetes and pancreases and hearts of infants who died of coxsackieviral myocarditis. *Diabetologia* 1990;**33**:290–298.
3. Iwasaki T, Monma N, Satodate R, Kawana R, Kurata T. An immunofluorescent study of generalized Coxsackie virus B3 infection in a newborn infant. *Acta Pathol Jap* 1985;**35**:741–748.
4. Gaaloul I, Riabi S, Harrath R, Hunter T, Hamda KB, Ghzala AB, Huber S, Aouni M. Coxsackievirus B detection in cases of myocarditis, myopericarditis, pericarditis and dilated cardiomyopathy in hospitalized patients. *Mol Med Rep* 2014;**10**:2811–2818.
5. Selinka HC, Wolde A, Sauter M, Kandolf R, Klingel K. Virus-receptor interactions of coxsackie B viruses and their putative influence on cardiotropism. *Med Microbiol Immunol* 2004;**193**:127–131.
6. Klingel K, Rieger P, Mall G, Selinka HC, Huber M, Kandolf R. Visualization of enteroviral replication in myocardial tissue by ultrastructural in situ hybridization: identification of target cells and cytopathic effects. *Lab Invest* 1998;**78**:1227–1237.
7. Klingel K, Stephan S, Sauter M, Zell R, McManus BM, Bultmann B, Kandolf R. Pathogenesis of murine enterovirus myocarditis: virus dissemination and immune cell targets. *J Virol* 1996;**70**:8888–8895.
8. Martino TA, Liu P, Sole MJ. Viral infection and the pathogenesis of dilated cardiomyopathy. *Circ Res* 1994;**74**:182–188.
9. Massilamany C, Gangaplara A, Reddy J. Intricacies of cardiac damage in coxsackievirus B3 infection: implications for therapy. *Int J Cardiol* 2014;**177**:330–339.
10. Bouin A, Nguyen Y, Wehbe M, Renois F, Fornes P, Bani-Sadr F, Metz D, Andreoletti L. Major persistent 5′ terminally deleted coxsackievirus B3 populations in human endomyocardial tissues. *Emerg Infect Dis* 2016;**22**:1488–1490.
11. Kaese S, Larbig R, Rohrbeck M, Frommeyer G, Dechering D, Olligs J, Schonhofer-Merl S, Wessely R, Klingel K, Seebohm G, Eckardt L. Electrophysiological alterations in a murine model of chronic coxsackievirus B3 myocarditis. *PLoS One* 2017;**12**:e0180029.
12. Pauschinger M, Phan MD, Doerner A, Kuehl U, Schwimmbeck PL, Poller W, Kandolf R, Schultheiss HP. Enteroviral RNA replication in the myocardium of patients with left ventricular dysfunction and clinically suspected myocarditis. *Circulation* 1999;**99**:889–895.
13. Kilbourne ED, Wilson CB, Perrier D. The induction of gross myocardial lesions by a Coxsackie (pleurodynia) virus and cortisone. *J Clin Invest* 1956;**35**:362–370.
14. Grodums EI, Dempster G. Myocarditis in experimental Coxsackie B-3 infection. *Can J Microbiol* 1959;**5**:605–615.
15. Klingel K, Hohenadl C, Canu A, Albrecht M, Seemann M, Mall G, Kandolf R. Ongoing enterovirus-induced myocarditis is associated with persistent heart muscle infection: quantitative analysis of virus replication, tissue damage, and inflammation. *Proc Natl Acad Sci USA* 1992;**89**:314–318.
16. Rabin ER, Hassan SA, Jenson AB, Melnick JL. Coxsackie virus B3 myocarditis in mice. An electron microscopic, immunofluorescent and virus-assay study. *Am J Pathol* 1964;**44**:775–797.
17. Li M, Wang X, Xie Y, Xie Y, Zhang X, Zou Y, Ge J, Chen R. Initial weight and virus dose: two factors affecting the onset of acute coxsackievirus B3 myocarditis in C57BL/6 mouse—a histopathology-based study. *Cardiovasc Pathol* 2013;**22**:96–101.
18. Tracy S, Höfling K, Pirruccello S, Lane PH, Reyna SM, Gauntt CJ. Group B coxsackievirus myocarditis and pancreatitis: connection between viral virulence phenotypes in mice. *J Med Virol* 2000;**62**:70–81.
19. Slifka MK, Pagarigan R, Mena I, Feuer R, Whitton JL. Using recombinant coxsackievirus B3 to evaluate the induction and protective efficacy of CD8+ T cells during picornavirus infection. *J Virol* 2001;**75**:2377–2387.
20. Leipner C, Grün K, Schneider I, Glück B, Sigusch HH, Stelzner A. Coxsackievirus B3-induced myocarditis: differences in the immune response of C57BL/6 and Balb/c mice. *Med Microbiol Immunol* 2004;**193**:141–147.

21. Schmidtke M, Merkle I, Klingel K, Hammerschmidt E, Zautner AE, Wutzler P. The viral genetic background determines the outcome of coxsackievirus B3 infection in outbred NMRI mice. *J Med Virol* 2007;**79**:1334–1342.
22. Kallewaard NL, Zhang L, Chen JW, Guttenberg M, Sanchez MD, Bergelson JM. Tissue-specific deletion of the coxsackievirus and adenovirus receptor protects mice from virus-induced pancreatitis and myocarditis. *Cell Host Microb* 2009;**6**:91–98.
23. Persichino J, Garrison R, Krishnan R, Sutjita M. Effusive-constrictive pericarditis, hepatitis, and pancreatitis in a patient with possible coxsackievirus B infection: a case report. *BMC Infect Dis* 2016;**16**:375.
24. Knowlton KU, Jeon ES, Berkley N, Wessely R, Huber S. A mutation in the puff region of VP2 attenuates the myocarditic phenotype of an infectious cDNA of the Woodruff variant of coxsackievirus B3. *J Virol* 1996;**70**:7811–7818.
25. Fechner H, Sipo I, Westermann D, Pinkert S, Wang X, Suckau L, Kurreck J, Zeichhardt H, Muller O, Vetter R, Erdmann V, Tschope C, Poller W. Cardiac-targeted RNA interference mediated by an AAV9 vector improves cardiac function in coxsackievirus B3 cardiomyopathy. *J Mol Med* 2008;**86**:987–997.
26. Spur EM, Althof N, Respondek D, Klingel K, Heuser A, Overkleeft HS, Voigt A. Inhibition of chymotryptic-like standard proteasome activity exacerbates doxorubicin-induced cytotoxicity in primary cardiomyocytes. *Toxicology* 2016;**353–354**:34–47.
27. Knoch KP, Bergert H, Borgonovo B, Saeger HD, Altkruger A, Verkade P, Solimena M. Polypyrimidine tract-binding protein promotes insulin secretory granule biogenesis. *Nat Cell Biol* 2004;**6**:207–214.
28. Hovi T, Roivainen M. Peptide antisera targeted to a conserved sequence in poliovirus capsid VP1 cross-react widely with members of the genus *Enterovirus*. *J Clin Microbiol* 1993;**31**:1083–1087.
29. Hvid H, Klopfleisch R, Vienberg S, Hansen BF, Thorup I, Jensen HE, Oleksiewicz MB. Unique expression pattern of the three insulin receptor family members in the rat mammary gland: dominance of IGF-1R and IRR over the IR, and cyclical IGF-1R expression. *J Appl Toxicol* 2011;**31**:312–328.
30. Szalay G, Sauter M, Hald J, Weinzierl A, Kandolf R, Klingel K. Sustained nitric oxide synthesis contributes to immunopathology in ongoing myocarditis attributable to interleukin-10 disorders. *Am J Pathol* 2006;**169**:2085–2093.
31. Pappritz K, Savvatis K, Miteva K, Kerim B, Dong F, Fechner H, Muller I, Brandt C, Lopez B, Gonzalez A, Ravassa S, Klingel K, Diez J, Reinke P, Volk HD, van Linthout S, Tschope C. Immunomodulation by adoptive regulatory T-cell transfer improves Coxsackievirus B3-induced myocarditis. *FASEB J* 2018;fj201701408R. doi: 10.1096/fj.201701408R.
32. Geisler A, Schön C, Größl T, Pinkert S, Stein EA, Kurreck J, Vetter R, Fechner H. Application of mutated miR-206 target sites enables skeletal muscle-specific silencing of transgene expression of cardiotropic AAV9 vectors. *Mol Ther* 2013;**21**:924–933.
33. Stein EA, Pinkert S, Becher PM, Geisler A, Zeichhardt H, Klopfleisch R, Poller W, Tschope C, Lassner D, Fechner H, Kurreck J. Combination of RNA interference and virus receptor trap exerts additive antiviral activity in coxsackievirus B3-induced myocarditis in mice. *J Infect Dis* 2015;**211**:613–622.
34. Pinkert S, Westermann D, Wang X, Klingel K, Dörner A, Savvatis K, Größi T, Krohn S, Tschöpe C, Zeichhardt H, Kotsch K, Weitmann K, Hoffmann W, Schultheiss H-P, Spiller OB, Poller W, Fechner H. Prevention of cardiac dysfunction in acute coxsackievirus B3 cardiomyopathy by inducible expression of a soluble coxsackievirus-adenovirus receptor. *Circulation* 2009;**120**:2358–2366.
35. Meldrum DR. Tumor necrosis factor in the heart. *Am J Physiol* 1998;**274**:R577–R595.
36. van Linthout S, Tschöpe C. Inflammation–cause or consequence of heart failure or both? *Curr Heart Fail Rep* 2017;**14**:251–265.

Translational perspective

The use of H3N-375TS will allow the investigation of the pathogenesis of coxsackievirus B3 (CVB3) myocarditis independently of severe systemic CVB3 infection and pancreatitis. It may also be a superior alternative for the study of new treatments in the post-viraemia phase of CVB3-induced myocarditis.